

Galactic Chemical Evolution of the Lighter Neutron Capture Elements Sr, Y and Zr *

Cui-Hua Du^{1,2}, Bo Zhang^{1,3}, Han-Feng Song¹ and Qiu-He Peng⁴

¹ Department of Physics, Hebei Normal University, Shijiazhuang 050016;
dch@vega.bac.pku.edu.cn; zhangbo@hebtu.edu.cn

² National Astronomical Observatory, Chinese Academy of Science, Beijing 100012

³ Center of Theoretical Nuclear Physics, National Laboratory of Heavy Ion Accelerator, Lanzhou 730000

⁴ Department of Astronomy, Nanjing University, Nanjing 210093

Received 2002 December 10; accepted 2003 May 15

Abstract Based on a three-component Galaxy chemical evolutionary model satisfying a large set of Galactic and extragalactic constraints, we compute the chemical evolution of the lighter neutron capture elements (e.g., Sr, Y and Zr) taking into account contributions from three processes. We compare our model results with available observational results and find that the observed trends can be understood in the light of present knowledge of neutron capture nucleosynthesis.

Key words: stars: AGB and post-AGB — Galaxy: halos — ISM:abundances

1 INTRODUCTION

The abundance distributions of n-capture elements can provide direct and detailed information on the nucleosynthesis in every stage after the formation of the galaxies. Furthermore, it can put more accurate constraints on the chemical evolution of the Galaxy. The n-capture elements are synthesized by slow and rapid n-capture processes (the so-called s- and r-processes). The s-process is further divided into two categories: the main s-component and the weak s-component. The main s-component is usually considered to be active during the double-shell burning phase of low mass ($1 - 3M_{\odot}$) and intermediate-mass ($4 - 7M_{\odot}$) AGB stars. The weak s-component, which has been suggested to be active during the core He burning in massive stars with $M \geq 10M_{\odot}$, is responsible for the production of the lighter elements, such as Sr, Y, and Zr.

The study of the Galactic evolution of the heavier elements produced by the s- and r-processes has been addressed in previous investigations. For example, under the crude assumption that the production of a given s-isotope in a simple one-zone model, Mathews (1992) studied the chemical evolution of neutron capture elements and provided insight into the kinds

* Supported by the National Natural Science Foundation of China.

of stellar environment responsible for the r- and s-process nucleosynthesis. Pagel et al. applied an analytical model of chemical evolution in the Galactic disk to study r- and s-process element abundance distributions (Pagel 1997), and they treated the s-process as the primary process and considered its production as constant. With the available quantitative yields from detailed nucleosynthesis calculations for different masses and metallicities, Travaglio calculated the evolution of n-capture elements from Ba to Eu and Pb in the interstellar medium (ISM) of the Galaxy (Travaglio 1999, 2001). Up to now, the abundance of the heavier n-capture elements can be understood with the early r-process in the history of the Galaxy and with s-process contribution occurring at higher metallicities or later times. Observational results have shown that the r-process abundances of the solar system cannot be used to explain the origin of the lighter ($Z < 56$) n-capture elements in metal-poor stars. As for high metallicities, the abundance distribution of the elements Sr, Y and Zr cannot be interpreted only by the s-process (Zhang 1999). Although some observational results of the abundance distribution of metal-poor stars have been obtained, only the r-process contribution to the element Sr in the Galactic halo has been studied (Travaglio 2001). Since it can provide a direct handle on the nucleosynthesis in every stage after the formation of galaxies, it is very important to determine the abundance distribution of the heavy elements.

We consider the weak s-process contribution to the lighter n-capture elements, and concentrate on the abundances distribution of Sr, Y and Zr, and compare them with the available observational data.

2 MODEL AND BASIC EQUATION

2.1 Multiphase Evolution of Three-Component Galaxy

The aim of galactic chemical evolution models is to reproduce the abundance pattern observed in the Galaxy as well as in external galaxies. The abundance distribution function is one of the most fundamental local observational constraints on the theory of Galactic chemical evolution. In recent years, it becomes more important and active in the field of galactic chemical evolution (Chang 1999, 2002; Liang 2000; Hou 2000, 2001, 2002), and enters into other aspects of galaxy formation and evolution. We adopt the Galactic chemical evolution models (Pardi et al. 1995; Travaglio et al. 1999), and the Galaxy is divided into three components: a halo, a thick disk and a thin disk. In each component, matter is assumed to be represented by diffuse gas (g), molecular clouds (c), stars of both low (s_1) and high masses (s_2 ; $M > 4M_\odot$), and the remnants (r). The model is based on a self-regulated picture of star formation. It is assumed that the Galaxy disk is sheet-like, which originates and grows from the infall of a thick disk and halo, and that no radial flow is considered.

In the following equations, the suffix j refers to the different zones: $j = H$ for the halo, T for the thick disk, and D for the thin disk. The indices 1 and 2 refer to the low- and high-mass star ranges, respectively. The coupling of the components is described by the term F_j . In the element abundance equations, the term K_j denotes the infalling element abundance.

$$\begin{aligned}
 \frac{ds_{1,j}}{dt} &= H_{1,j}c_j^2 + a_{1,j}c_j s_{2,j} - D_{1,j}, \\
 \frac{ds_{2,j}}{dt} &= H_{2,j}c_j^2 + a_{2,j}c_j s_{2,j} - D_{2,j}, \\
 \frac{dg_j}{dt} &= -\mu_j g_j^n + a'_j c_j s_{2,j} + H'_j c_j^2 + F_j + W_j,
 \end{aligned} \tag{1}$$

$$\begin{aligned}\frac{dc_j}{dt} &= \mu_j g_j^n - (a_{1,j} + a_{2,j} + a'_j)c_j s_{2,j} - (H_{1,j} + H_{2,j} + H'_j)c_j^2, \\ \frac{dr_j}{dt} &= D_{1,j} + D_{2,j} - W_j, \\ \frac{dX_{i,j}}{dt} &= (W_{i,j} - X_{i,j}W_j + K_j)/(g_j + c_j).\end{aligned}$$

The processes and the relevant coefficients are as follows:

- (1) Star formation from cloud collisions in the three components, the halo, thick disk and thin disk: $H_{1,2,j}c_j^2$.
- (2) Induced star formation, via massive star-cloud interaction: $a_{1,2,j}c_j s_{1,2,j}$.
- (3) Cloud formation from the diffused gas: $\mu_j g_j^n$. Here, a power law with index $n = 1.5$ is adopted.

Here, the death (D_j) and restitution (W_j) terms are evaluated by taking into account the mass dependence of stellar lifetimes and nucleosynthesis.

$$\begin{aligned}D_{1,j}(t) &= \int_{m_{\min}}^{m^*} m\phi(m)\psi_j(t - \tau_m)dm, \\ D_{2,j}(t) &= \int_{m^*}^{m_{\max}} m\phi(m)\psi_j(t - \tau_m)dm, \\ W_j(t) &= \int_{m_l(t-\tau_m)}^{m_{\max}} \left[\sum_i Q_{ji}(m) \right] \phi(m)\psi_j(t - \tau_m)dm,\end{aligned}$$

where $\phi(m)$ is the initial mass function (IMF), $\psi(t)$ is the star formation rate (SFR), τ is the stellar lifetime, the restitution matrices $\sum_i Q_{ji}$ are defined as the fraction of mass of an element j initially present in a star with mass m that is transformed to element i and ejected. The coefficients $H_{1,2,j}$, $a_{1,2,j}$, a'_j , H'_j and μ_j depend on the IMF and the observational constraints. The total mass of the system ($H+T+D$) is chosen in accordance with the observational estimate of the present local surface mass density, chosen here to be $70 M_{\odot} \text{ pc}^{-2}$ (Bahcall 1984). The age of the Galaxy is assumed to be 14 Gyr (Rana 1991).

We will discuss the results for three different models or cases, labelled a, b and c. Cases a and b are both based on the initial mass function (IMF) of Kroupa (1993) and the main sequence lifetimes from Larson (1974) for case a, and those from Schaller (1992) for case b. Case c uses the same main sequence lifetimes as case a but with the Salpeter (1955) IMF.

2.2 Main-sequence Lifetimes

In cases a and c, the adopted relation between the main sequence lifetime τ_m (in units of Gyr) and the initial mass m (in units of M_{\odot}) is (Larson 1974)

$$\log m = 1.983 - 1.054\sqrt{(\log \tau_m + 2.52)}. \quad (2)$$

For the sake of simplicity, it is assumed that, except for Type Ia Supernova (Type Ia SNe) stars, all stars evolve as single stars even if they are members of binary systems. All massive stars ($m > 9M_{\odot}$) explode as Type II supernovae (Type II SNe), leaving behind a neutron star of mass $M_r = 0.5M_{\odot}$, and all intermediate and low mass stars ($m < 9M_{\odot}$) end up as white dwarfs. Type Ia SNe are thought to originate from carbon deflagration in C-O white dwarfs in

binary systems. The method of calculation of Type Ia SNe is the same as in Greggio (1983) and in Chang (1999). For case b, the lifetimes of massive stars are given directly by the stellar evolution calculations of Timmes et al. (1995). For stars with masses less than $11M_{\odot}$, we adopt the main-sequence lifetimes given by Schaller et al. (1992).

2.3 Initial Mass Function (IMF)

The adopted stellar initial mass function (IMF) in cases a and b is taken from Kroupa (1993), in which the IMF is described by a three-slope power law, $\phi(m) \propto m^{-(1+x)}$, with a relatively steep slope of $x = 1.7$ in the high-mass region ($m > 1M_{\odot}$), a flattening to $x = 1.2$ in the low-mass range ($0.5M_{\odot} \leq m \leq 1.0M_{\odot}$) and further to $x = 0.3$ for $m < 0.5M_{\odot}$. The Salpeter (1955) IMF is adopted in case c. Again, for consistency, we adopt the same IMF for the halo and the thick disk.

2.4 Star Formation Rate (SFR)

In the present paper, the star formation rates in the three components are determined self-consistently by the phase evolution

$$\psi_H(t) = (H_{1H} + H_{2H})c_H^2 + (a_{1H} + a_{2H})c_H s_{2H},$$

$$\psi_T(t) = (H_{1T} + H_{2T})c_T^2 + (a_{1T} + a_{2T})c_T s_{2T},$$

$$\psi_D(t) = (H_{1D} + H_{2D})c_D^2 + (a_{1D} + a_{2D})c_D s_{2D}.$$

2.5 Comparison between Model Results and Observational Constraints

A successful model of Galactic chemical evolution should reproduce the main observational features of the solar neighborhood. These constraints include:

- (1) the characteristic parameters of metallicity in the three components (Table 1);
- (2) the local surface mass density, SFR and mass ratio of the three components in the solar neighborhood (Table 2);
- (3) the observed age-metallicity relation (AMR) and data in the references (Edvardsson 1993; Rocha 2000);
- (4) the G dwarfs metallicity distribution in the solar neighborhood;
- (5) the correlation between [O/Fe] and [Fe/H] and observed data in the references (Edvardsson 1993; Chen 2000; Barbuy 1989).

Table 1 Observed and Predicted Metallicity

	Halo			Thick Disk			Thin Disk		
	[Fe/H] _m	[Fe/H] _M	⟨[Fe/H]⟩	[Fe/H] _m	[Fe/H] _M	⟨[Fe/H]⟩	[Fe/H] _m	[Fe/H] _M	⟨[Fe/H]⟩
observation	-4	0	-1.5	-1.4	0	-0.6	-0.8	0.2	-0.1
case a	-4	0.2	-1.5	-2.6	0.2	-1.0	-1.4	0.4	-0.1
case b	-3.4	0.4	-1.6	-2.6	0.4	-1.2	-2	0.4	-0.6
case c	-4	-0.4	-1.6	-3.4	-0.4	-1.3	-1.4	0.4	-0.6

In Table 1, we list the characteristic values of iron abundance, the minimum [Fe/H]_m, the maximum [Fe/H]_M and the average ⟨[Fe/H]⟩, in the three components for the three different cases studied. In Table 2, we compare the observed and predicted local surface mass density, SFR and mass ratio of the three components. The parameters compared are the surface mass density of gas (σ_g); the surface mass density of stars (σ_*); the surface mass density of remnant

(σ_{rem}); the ratio between the surface mass density of gas and the total mass ($\sigma_g/\sigma_{\text{total}}$); the relative normalization of the halo, thick disk and thin disk surface mass densities ($M_H : M_T : M_D$).

The model parameters are adjusted to these observational constraints, i.e., the choice of parameters is not completely free because their values are strongly constrained by observational features in the solar neighborhood. Moreover, combinations of parameters are important in determining the observational constraints. In Fig. 1, the star formation histories in the three components for the three different cases are presented. As Fig. 1 shows, there are no very big differences in the three cases, but the result in case a is in closer agreement with that of the literature (Travaglio 1999).

The age-metallicity relation of field stars in the solar neighborhood is one of the most important constraints on the Galactic chemical evolution model. The age-metallicity relation in the thin disk for the three different cases is presented in Fig. 2. It shows the general trend that, of the three cases, the agreement between the model and observation is closest in cases a. However, because of the uncertainties in the derivation of the stellar ages, particularly for metal-poor stars, the derived age-metallicity relation is limited (Pardi 1995) in that there exists a scatter in the iron abundance at early age for the metal-poor stars.

Table 2 Predicted and Observed Parameters of Three Models

	case a	case b	case c	observed	reference
$\sigma_g(M_\odot \text{ pc}^{-2})$	12.6	18.4	16	7 – 13	Dickey 1993
$\sigma_*(M_\odot \text{ pc}^{-2})$	37.1	32.5	34	30 – 40	Gilmore 1989
$\sigma_{\text{rem}}(M_\odot \text{ pc}^{-2})$	2.3	4.6	4.3	2 – 4	Mera 1998
$\sigma_g/\sigma_{\text{total}}$	0.18	0.26	0.23	0.05 – 0.2	Mera 1998
$\text{SFR}(M_\odot \text{ pc}^{-2})$	2.2	4	4	2 – 10	Guesten 1982
$M_H : M_T : M_D$	1:4:28	1:8:24	1:7:25	1:3:33	Kuijken 1989

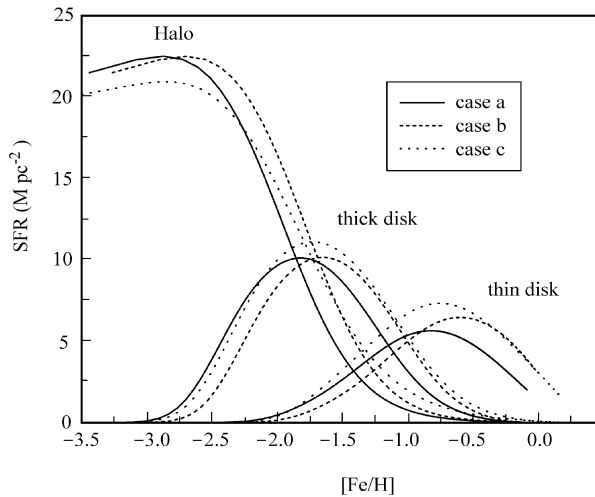


Fig. 1 Star formation rate ($M_\odot \text{ pc}^{-2} \text{ Gyr}^{-1}$) vs. $[\text{Fe}/\text{H}]$ in the halo, thick disk, and thin disk for case a (solid line), b (dashed line) and c (dotted line).

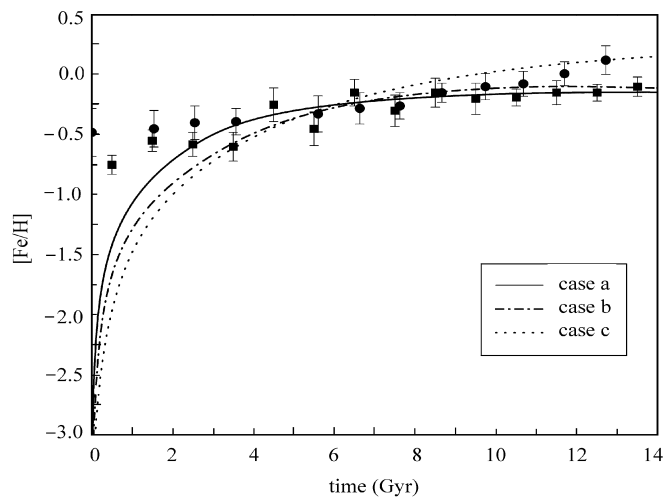


Fig. 2 $[\text{Fe}/\text{H}]$ vs. time (Gyr) in the thin disk for case a (solid line), b (dot dashed line) and c (dotted line). Observed data are taken from Edvardsson (1993, filled squares) and Rocha (2000, filled circles).

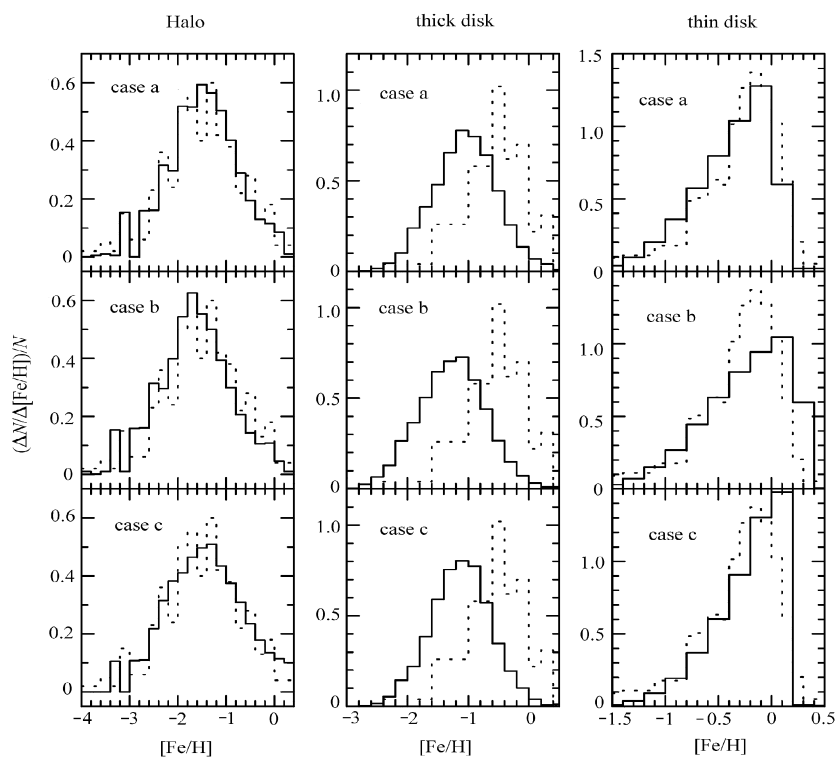


Fig. 3 G dwarfs distribution as a function of $[\text{Fe}/\text{H}]$ in the halo, thick disk and thin disk for three different cases. Observed data (dotted line) are taken from Sandage(1987) for the halo and thick disk, and from Chang (1998) for the thin disk.

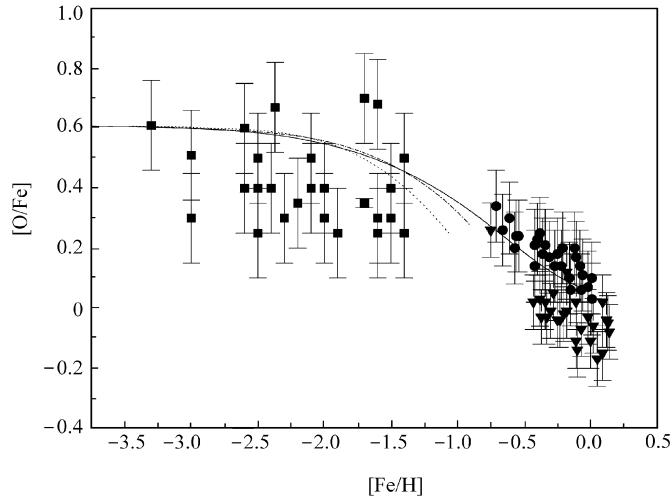


Fig. 4 [O/Fe] vs. [Fe/H] in the halo (dotted line), thick disk (dashed dot line), and thin disk (solid line). Observed data are taken from Barbuy (1989, filled squares), Chen (2000, filled circles), Edvardsson (1993, filled triangles).

Another important observational constraint is the metallicity distribution of G dwarfs in the solar neighborhood. Since G dwarfs have lifetimes greater than or equal to the age of the Galaxy, and hence can provide a complete record of the chemical evolutionary history. Figure 3 shows the G dwarfs distribution in the halo, thick disk and thin disk for the three different cases. The halo and thick disk distributions are compared with Sandage's data (Sandage 1987), while that of the thin disk, with Chang's data (Chang 1998). As shown in Fig. 3, the G dwarf distribution in case a is closest to the observed distribution and the predicted average iron value is $[\text{Fe}/\text{H}] \sim -1.5$ for the halo stars, $[\text{Fe}/\text{H}] \sim -1.0$ for the thick disk stars and $[\text{Fe}/\text{H}] \sim -0.2$ for the thin disk stars. In addition, it can be seen that even in case a there is still too many predicted low-metallicity stars (the G dwarfs problem) in the thick disk, this is probably due to the still too strong connection of the thick disk to the halo. It was in order to check the influence of the IMF on the metal enrichment that we computed our case c, assuming the Salpeter IMF, and the result is that for each of three components, the stars are more metal-poor in case c than in case a.

Evolution of the oxygen-to-iron ratio, [O/Fe], as a function of [Fe/H] for the best-fit model (case a), is shown in Fig. 4. The dot line shows the contribution of halo, the dash dot line, that of the thick disk and the solid line, that of the thin disk. As can be seen from the figure that there is a constant oxygen overabundance of 0.6 dex for $[\text{Fe}/\text{H}] < -2$ and the decline starts at $[\text{Fe}/\text{H}] > -2$. It shows that our model prediction is in good agreement with the observation and suggests that the main-sequence star lifetimes and IMF we adopted are reasonable.

3 RESULTS FOR THE GALACTIC EVOLUTION OF Sr, Y AND Zr

In this section we present our case a results for the evolution of the elements Sr, Y and Zr in the Galaxy. We consider the s-main and s-weak contributions as separate, and we compute the abundance of the elements resulting from the sum of the three processes and compare the model results with the observed data.

3.1 s-main Process Contribution

In the calculations, we adopt the production of s-main process nucleosynthesis (Liang 2000; Busso 2001) and we consider the contributions from 2 to $8M_{\odot}$ AGB stars. It is shown that the s-main process contribution dominates the Galactic chemical evolution of Sr, starting from $[\text{Fe}/\text{H}] \simeq -1.2$ in the thin disk. At such low metallicity, the contribution of s-process nucleosynthesis rapidly decreases with $[\text{Fe}/\text{H}]$. It can be due to the long lifetimes of low mass AGB stars, and the contribution resulting from more massive AGB stars is too small by far. Moreover, the stellar yields depend strongly on metallicity so that the low mass AGB stars do not contribute strongly to the observed abundances at low metallicity. We have also derived the resulting s-main component fractions (with respect to the corresponding solar abundances) at $t = t_{\odot}$, and this aspect will be further discussed below.

3.2 Contributions from the s-Weak Process and the r-Process

The weak s-process occurs during the core He-burning of massive stars with $M \geq 10M_{\odot}$, and the weak component mainly contribute to the lighter s-elements, like Sr, Y and Zr, etc. We adopt the yields from Prantzo (1990). Moreover, the s-weak contribution in the thin disk is higher than in the thick disk or halo. This can be explained thus: the yields depend strongly on the metallicity and rise with increasing metallicity, so the s-weak contribution in the thin disk is relatively high. Although the s-weak process contribution to very few or even none of the heavier n-capture elements, it is very important for our understanding of the nucleosynthesis of the lighter n-capture elements. As regards the r-process, we consider it to be a mechanism occurring primarily in Type II SNe with $15 - 25M_{\odot}$, as described by Travaglio (2001).

3.3 Contributions by the r-Process and s-Process to Galactic Chemical Evolution

In this section, we consider the r+s process contribution to the lighter n-capture elements and give the results for the Galactic chemical evolution of the elements Sr, Y and Zr. Figures 5–7 give the evolution of Sr, Y and Zr obtained by adding the r-, s-main and s-weak process contributions in the three Galactic components, and compare the model results with the observed data at different metallicities. The observed data are taken from the references (Hartmann 1988; Zhao 1990, 1993; Gratton 1988, 1994; Magain 1989; McWilliam 1998; Sean 2001). It can be seen from the figures that the $[\text{element}/\text{Fe}]$ begin to decline at $[\text{Fe}/\text{H}] \simeq -3.2$, due to a delay r-process production with respect to Fe, i.e., in the early times of the Galactic evolution more massive stars evolve quickly as SNe II Explosions, producing much of the O elements and some Fe, but little r-process elements. Later, with the increased metallicity, less massive stars ($15 - 25M_{\odot}$) explode as SNe II to produce r-process elements, so the abundance ratios $[\text{r-element}/\text{Fe}]$ rapidly increase. The curves are relatively smooth in the range $-2.8 \leq [\text{Fe}/\text{H}] \leq -1.2$, where r-process is dominant and s-process contributes relatively weakly. On the other hand, the s-process contribution begins gradually to take over at $[\text{Fe}/\text{H}] > -1.2$.

In Table 3 we give the resulting different process fractions (with respect to the corresponding solar abundances) at $t = t_{\odot}$ for case a. In columns (2), (3) and (4) we present the predicted main s-process, weak s-process and r-process contributions to Sr, Y and Zr and columns (5), (6) and (7) show the solar abundance of the three lighter n-capture elements from Käppeler (1989). From Table 3 we see that at $t = t_{\odot}$, for the Sr s-main fraction, the model prediction is 71% of the solar Sr abundance, the s-weak fraction is 13% and the r-fraction is 16%. Thus, constraints on the nucleosynthesis of the lighter n-capture element can be obtained in terms of the Galactic chemical evolution.

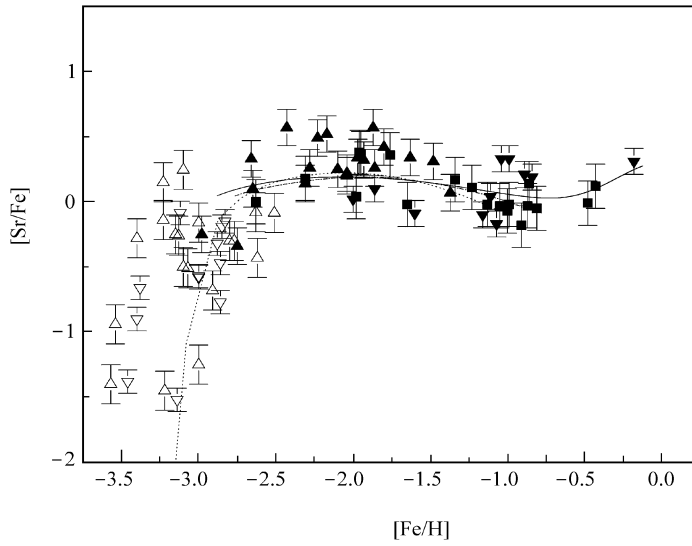


Fig. 5 Galactic evolution of $[\text{Sr}/\text{Fe}]$ as a function of $[\text{Fe}/\text{H}]$ in the halo (dotted line), thick disk (dashed dot line), and thin disk (solid line). Observational data are from: Hartmann (1988, filled downtriangles); Gratton (1988, open downtriangles); Zhao (1993, filled squares); Magain (1989, filled uptriangles).

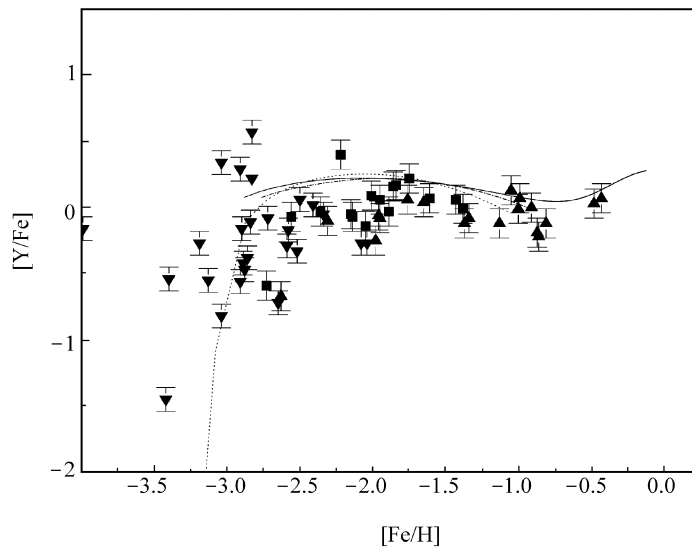


Fig. 6 Galactic evolution of $[\text{Y}/\text{Fe}]$ as function of $[\text{Fe}/\text{H}]$ in the halo (dotted line), thick disk (dashed dot line), and thin disk (solid line). Observational data are from: Zhao (1990, filled square); Zhao (1993, filled uptriangles); McWilliam (1998, filled downtriangles).

Table 3 Relative r- and s-process Contributions at $t = t_{\odot}$

Element	s-main	s-weak	r-	s-main(\odot)	s-weak(\odot)	r(\odot)
Sr	0.71	0.13	0.16	0.65	0.18	0.17
Y	0.78	0.07	0.18	0.81	0.15	0.04
Zr	0.69	0.03	0.28	0.66	0.07	0.27

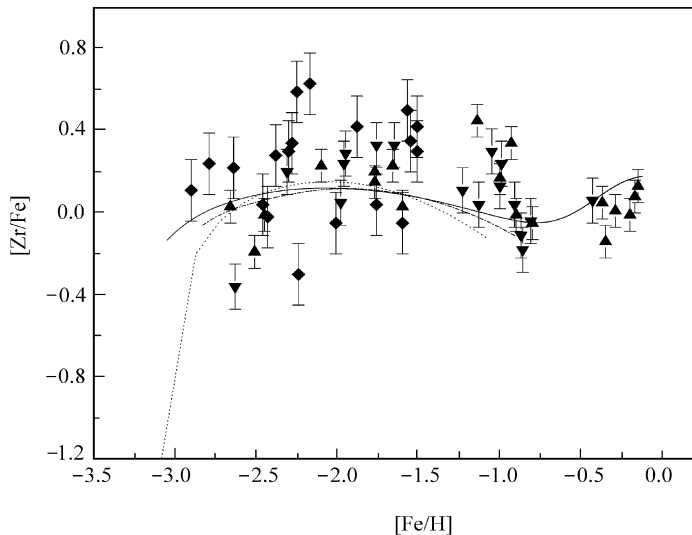


Fig. 7 Galactic evolution of $[Zr/Fe]$ as function of $[Fe/H]$ in the halo (dotted line), thick disk (dashed dot line), and thin disk (solid line). Observational data are from: Gratton (1994, filled uptriangles); Gilroy (1988, filled rhombs); Zhao (1993, filled downtriangles).

4 CONCLUSIONS AND DISCUSSION

On the basis of n-capture element nucleosynthesis scenario and the Galactic chemical evolution theory, we use a three-component, multi-phase chemical evolution model to calculate the evolution of the lighter n-capture elements Sr, Y and Zr. We discussed three different models and compared the calculated results with the observations. We can see from the calculated results that our adopted Galactic evolution model, case a, can reproduce some observed properties of the solar vicinity region. It proves that the adopted case a model is more reasonable than the other two cases. In addition, at higher metallicities, the s-weak process contribution of the lighter n-capture elements is not negligible, particularly for $[Fe/H] \geq -1.2$, where it plays a key role. When contributions from the s-main process, the s-weak process and the r-process contributions are considered, the abundances of the elements Sr, Y and Zr as functions of $[Fe/H]$ are found to be consistent with the metal-poor star observations. Taking into account the three processes in the Galaxy, we derive that their fractional contributions to Sr, Y and Zr at $t = t_{\odot}$ are in agreement with the solar system abundance results; this confirms the heavy elements

nucleosynthesis theory. In addition, it shows that the calculated method adopted in this paper is reasonable. The element Sr is an important lighter n-capture element, its s-weak process contribution from massive stars accounts for 13% of the solar composition of Sr, so that it can be used as a typical s-weak process element (Zhang 1999). It is significant to probe the weak s-process contribution to nucleosynthesis. However, at present, there are still some uncertainty in the Galactic evolution model and in the stellar nucleosynthesis production. In order to gain a true picture of heavy-element nucleosynthesis in metal-poor stars and the early history of the Galactic chemical evolution, more accurate observations would be useful to determine the relative contributions of the different processes to the n-capture elements. Moreover, the data of lighter n-capture elements, especially the abundance of elements with mass number A around 100, are also required to explore the contribution of the weak s-process. With improvements in these directions, the research of neutron-capture element abundance distribution and the Galaxy chemical evolution will provide more significant results that can be used in many aspects of nuclear astrophysics.

Acknowledgements We would like to thank the referee for his insightful comments and suggestion that improved this paper. We are also very grateful to Dr. Chenggang Shu and Dr. Ruixiang Chang for helping us to improve the paper. This work is supported by Chinese Academy of Sciences-Peking University Joint Beijing Astrophysical Center. This work is funded by Natural Science Foundation of China (Grant No. 19973002).

References

- Bahcall J. N., 1984, *ApJ*, 276, 169
Barbuy B., Erdelyi-Mendes M., 1989, *A&A*, 214, 239
Busso M., Gallino R., Lambert D. 2001, *ApJ*, 557, 802
Chang R. X., Hou J. L., Shu C. G., Fu C. Q., 1999, *A&A*, 350, 38
Chang R. X., Hou J. L., Fu C. Q., 1998, *Acta Astrophys. Sin.*, 18, 4
Chang R. X., Shu C. G., Hou J. L., 2002, *Chin. J. Astron. Astrophys.*, 2(1), 17
Chen Y. Q., Nissen P. E., Zhao G., 2000, *A&AS*, 141, 491
Cowan J. J., Burris D. L., Sneden C., 1995, *ApJ*, 439, 51
Dickey J. M., 1993, In: M. H. Roberts, ed., *ASP Conf. Ser. 39, The Minnesota Lectures on the Structure and Dynamics of the Milky Way*, San Francisco: ASP, p.93
Edvardsson B., Andersen J., Gustafsson B. et al., 1993, *A&A*, 275, 101
Gilmore G., Wyse R., Kuijen K., 1989, In: *Evolutionary Phenomena in Galaxies*, Cambridge: Cambridge Univ. Press, p.172
Gilroy K. K., Sneden C., Pilachowski C., 1988, *ApJ*, 327, 298
Gratton R. G., Sneden C., 1988, *A&A*, 204, 193
Gratton R. G., Sneden C., 1994, *A&A*, 287, 927
Greggio L., Renzini A., 1983, *A&A*, 338, 881
Guesten R., Mezger M., 1982, *Vistas in Astr.*, 26, 159
Hartmann K. L., Gehren T., *A&A*, 1988, 199, 269
Hou J. L., Prantzos N., Boissier S., 2000, *A&A*, 362, 921
Hou J. L., Chang R. X., Chen L., 2002, *Chin. J. Astron. Astrophys.*, 2, 226
Hou J. L., Chang R. X., 2001, *Progress in Astronomy*, 19, 1, 68
Käppeler F., Beer H., Wisshak K., *Rep. Prog. Phys.*, 1989, 52, 945
Kroupa P., Tout C., Gilmore G., 1993, *MNRAS*, 262, 545

- Kuijken K., Gilmore G., 1989, *MNRAS*, 239, 605
Larson R. B., 1974, *MNRAS*, 166, 585
Liang Y. C., Zhao G., Zhang B., 2000, *A&A*, 363, 555
Mathews G. J., Bazan G., Cowan J. J., 1992, *ApJ*, 391, 719
Magain P., 1989, *A&A*, 209, 211
McWilliam A., 1998, *ApJ*, 115, 1640
Mera D., Chabrier G., Schaeffer R., 1998, *A&A*, 330, 937
Pagel B. E. J., Tautvaisiene G., 1997, *MNRAS*, 288, 108
Pardi M. C., Ferrini F., Matteucci F., 1995, *ApJ*, 444, 207
Prantzos N., Hashimoto M., Nomoto K., 1990, *A&A*, 234, 211
Rana N. C., 1991, *ARA&A*, 29, 129
Rocha-Pinto H. J., Maciel W. J., Scalo J., Chiappini C., 2000, *ApJ*, 358, 850
Ryan S. G., Aoki W. et al., 2001, *Memorie della Societa Astronomica Italiana*, 72, 337
Sandage A., Fouts G., 1987, *AJ*, 93, 610
Salpeter E. E., 1955, *ApJ*, 121, 161
Schaller G., Schaerer D., Meynet G. et al., 1992, *A&AS*, 96, 269
Timmes F. X., Woosley S. E., Weaver T. A., 1995, *ApJS*, 98, 617
Travaglio C., Galli D., Gallino R. et al., 1999, *ApJ*, 521, 691
Travaglio C., Galli D., Gallino R. et al., 2001, *ApJ*, 547, 217
Zhang Bo, Li Ji, Zhang Caixia, 1999, *ApJ*, 513, 910
Zhang Bo, Zhang Caixia, Li Ji, et al., 1999, *Science in China (Series A)*, 42, 401
Zhao G., Magain P., 1990, *A&A*, 238, 242
Zhao G., *Acta Astrophys. Sin.*, 1993, 13(4), 347